https://doi.org/10.5607/en21027
Exp Neurobiol. 2022 Apr;31(2):105-115.
pISSN 1226-2560 • eISSN 2093-8144

Original Article

Experimental Neurobiology

Time Course of Remote Neuropathology Following Diffuse Traumatic Brain Injury in the Male Rat

Katherine R. Giordano[1,2,3†], L. Matthew Law[1,2,3†], Jordan Henderson[1,2], Rachel K. Rowe[4] and Jonathan Lifshitz[1,2,3*]

[1]BARROW Neurological Institute at Phoenix Children's Hospital, Phoenix, AZ 85013, [2]Department of Child Health, University of Arizona College of Medicine – Phoenix, Phoenix, AZ 85004, [3]Phoenix Veterans Affairs Health Care System, Phoenix, AZ 85012, [4]Department of Integrative Physiology, University of Colorado, Boulder, CO 80309, USA

Traumatic brain injury (TBI) can affect different regions throughout the brain. Regions near the site of impact are the most vulnerable to injury. However, damage to distal regions occurs. We investigated progressive neuropathology in the dorsal hippocampus (near the impact) and cerebellum (distal to the impact) after diffuse TBI. Adult male rats were subjected to midline fluid percussion injury or sham injury. Brain tissue was stained by the amino cupric silver stain. Neuropathology was quantified in sub-regions of the dorsal hippocampus at 1, 7, and 28 days post-injury (DPI) and coronal cerebellar sections at 1, 2, and 7 DPI. The highest observed neuropathology in the dentate gyrus occurred at 7 DPI which attenuated by 28 DPI, whereas the highest observed neuropathology was at 1 DPI in the CA3 region. There was no significant neuropathology in the CA1 region at any time point. Neuropathology was increased at 7 DPI in the cerebellum compared to shams and stripes of pathology were observed in the molecular layer perpendicular to the cerebellar cortical surface. Together these data show that diffuse TBI can result in neuropathology across the brain. By describing the time course of pathology in response to TBI, it is possible to build the temporal profile of disease progression.

Key words: Traumatic brain injury, Neuropathology, Diffuse axonal injury, Silver stain, Hippocampus, Cerebellum

INTRODUCTION

Traumatic brain injury (TBI) is an event which leads to physiological processes that can result in lifelong consequences [1]. The heterogeneity of TBI makes each injury, response, and recovery course unique to the millions of people impacted by TBI each year [1]. TBI can be categorized as focal or diffuse, the latter being more common, although combinations of focal/diffuse injury occur [2]. Diffuse TBI is characterized by a mechanical force exerted on the head or skull, followed by acceleration and deceleration of the brain within the skull [2]. The acceleration/deceleration of the brain produces the mechanical injury and occurs immediately after impact, which shears axons and disrupts circuits [2]. Ensuing neuropathological signaling goes on to restore brain homeostasis, but this process often exacerbates the TBI [3]. Post-traumatic pathology encompasses myelin loss, glial activation, cytokine production, reactive oxygen species production and can occur minutes to days to weeks after the mechanical event [2]. TBI neuropathology is a driving force of both acute deficits and chronic morbidities, which can include clinical symptoms in the domains of cognition, somatosensation, and movement that can persist for years following the injury [4-6].

Although there is no overt cell loss in diffuse TBI, there is extensive diffuse injury throughout the brain in the form of disrupted connections and damaged axonal processes [7-9]. One method that has been widely used to assess neuropathology in TBI and

Submitted December 15, 2021, Revised December 15, 2021,
Accepted April 12, 2022

*To whom correspondence should be addressed.
TEL: 1-602-827-2346
e-mail: jlifshitz@email.arizona.edu
†These authors contributed equally to this article.

other neurodegenerative disease is the amino cupric silver staining technique [10-12]. The silver staining technique was first used to visualize dendritic and axonal processes in the early 1900's. The staining quality was non-specific and labeled both healthy and degenerating neuronal processes [10, 13, 14]. Later modifications to the silver stain protocol amplified staining of degenerative processes and reduced staining of healthy processes, resulting in a more discrete delineation of pathology [10, 15]. While neurodegeneration is a component of neuropathology and can result in full degeneration of a cell [10, 11], it is important to note that positive silver staining does not always indicate assured neuronal death, but could represent axotomy, neurofilament compaction, or synaptic sprouting. Positive silver staining is associated with mechanical injury, pathological processes, and circuit reorganization, and therefore cannot distinguish specific processes of pathology. For example, diffuse TBI in the rodent somatosensory cortex resulted in neuronal atrophy in the somatosensory cortex compared to sham controls at 7 days post-injury (DPI), but neuronal nuclear volume returned to sham control levels at 28 DPI [11]. The associated silver staining showed a time course with the highest level of silver staining at 7 DPI that was not fully resolved by 28 DPI [11]. Based on these data, we used the de Olmos amino cupric silver stain for histological representation of neuropathology in various brain regions after TBI [10-12].

We have previously reported the progression of neuropathology in cortex, thalamus, midbrain, and brainstem using the de Olmos amino cupric silver technique [11, 16-19]. Archived tissue provides an opportunity to extend the investigations of neuropathology to new brain regions. To date, no quantification of neuropathology following midline fluid percussion injury in the rodent in the three major sub-regions of the dorsal hippocampus or the cerebellum over time has been done. Therefore, the current study sought to categorize progressive neuropathology in the dorsal hippocampus and cerebellum following experimental diffuse TBI using the de Olmos amino cupric silver stain method.

MATERIALS AND METHODS

All animal studies were conducted in accordance with the guidelines established by the internal IACUC (Institutional Animal Care and Use Committee) at the University of Kentucky and the NIH guidelines for the care and use of laboratory animals. Studies are reported following the ARRIVE (Animal Research: Reporting In Vivo experiments) guidelines [20]. Randomization of animals was achieved by assigning animals to brain injury groups before the initiation of the study to ensure equal distribution across groups. Data collection stopped at pre-determined final endpoints based on days post-injury (DPI) for each animal. Animals were excluded from the study if post-operative weight decreased by 15% of pre-surgical weight (n=0). All animal quantification of silver stain was scored by investigators blinded to the treatment groups. Data sets were screened using the extreme studentized deviate method for significant outliers.

Animals

Adult male Sprague Dawley rats (n=15, 300~350 g; Harlan, IN) were used for all experiments. Rats were housed in pairs in a 12 h light:12 h dark cycle at a constant temperature (23±2℃) with food and water available *ad libitum* according to the Association for Assessment and Accreditation of Laboratory Animal Care International. Rats were acclimated to their environment following shipment for at least 1 week before any experiments. After surgery, rats were evaluated daily for postoperative care by a physical examination and documentation of each animal's condition.

Midline fluid percussion injury

Rats were subjected to midline fluid percussion injury (mFPI) consistent with methods described previously [21-24]. Rats were anesthetized using 5% isoflurane in 100% oxygen for 5 minutes and the head of the rat was placed in a stereotaxic frame with continuously delivered isoflurane at 2.5% via nosecone. Rats were anesthetized with 5% isoflurane, transferred to a stereotaxic frame (Kopf Instrument, Tujunga, CA), and maintained at 2% isoflurane via a nose cone for the duration of the surgery. During surgery, body temperature was maintained at 37℃ with an isothermal heating pad (Braintree Scientific). A midline incision was made exposing bregma and lambda, and fascia was removed from the surface of the skull. A trephine (4.8 mm outer diameter) was used for the craniectomy, centered on the sagittal suture between bregma and lambda without disruption of the dura. A skull screw was secured in a 1-mm hand-drilled hole into the right frontal bone. An injury cap prepared from the female portion of a Luer-Loc needle hub was fixed over the craniectomy using cyanoacrylate gel and methyl-methacrylate (Hygenic Corp, Akron, OH). The incision was sutured at the anterior and posterior edges and topical Lidocaine ointment was applied. Rats were placed in a heated recovery cage and monitored until ambulatory.

For injury induction, rats were re-anesthetized (60~90 min after surgery) with 5% isoflurane delivered for 5 minutes. The dura was visually inspected through the hub to make sure it was intact with no debris. The hub was then filled with normal saline and attached to the male end of the fluid percussion device (Custom Design and Fabrication, Virginia Commonwealth University, Richmond, VA). A diffuse brain injury (1.8~2.0 atm) was administered by releasing

https://doi.org/10.5607/en21027

the pendulum onto the fluid-filled cylinder. Sham-injured rats underwent the same surgical procedures except the pendulum was not released. Rats were monitored for the presence of a forearm fencing response, and righting reflex times were recorded for the injured rats as indicators of injury severity [25]. The righting reflex time is the total time from the initial impact until the rat spontaneously rights itself from a supine position. The fencing response is a tonic posturing characterized by extension and flexion of opposite arms that has been validated as an overt indicator of injury severity [25]. The injury hub was removed, and the brain was inspected for uniform herniation and integrity of the dura. The dura was intact in all rats and none were excluded. The incision was cleaned using saline and closed using staples. Diffuse brain-injured rats had righting reflex recovery times between 5~10 minutes and a positive fencing response. Sham-injured rats recovered a righting reflex within 20 seconds. After spontaneously righting, rats were placed in a heated recovery cage and monitored until ambulatory (approximately 5~15 minutes) before being returned to their cage. Adequate measures were taken to minimize pain or discomfort.

Tissue preparation

At selected time points (1, 2, 7, 28 DPI) or sham operation, rats were given an overdose of sodium pentobarbital (i.p.) and transcardially perfused with 4% paraformaldehyde after a phosphate buffered saline flush. The brains were transferred to fresh fixative solution and sent to NeuroScience Associates Inc. (Knoxville, TN) to be processed for histological and immunohistochemical staining. The brains were embedded into a gelatin matrix where they could be frozen and sectioned from one solid block (MultiBrain® Technology, NeuroScience Associates). MultiBrain® Technology processes up to 16 rat brains simultaneously, which results in uniform staining across sections, concurrent staining in adjacent sections, and built-in quality control. Sections of 40 μm thickness were taken in the coronal plane and wet-mounted on 2% gelatin-subbed slides.

Amino cupric silver technique and analysis

Neuropathology, indicated by argyrophilic reaction product, was examined using de Olmos amino cupric silver stain technique according to proprietary protocols [10, 26-28]. Brain sections were counterstained with Neutral Red to stain normal cell bodies. Both stained and unstained brain sections were returned to our laboratory. The same histological series has been incorporated into other published datasets [11, 29-34] and analyzed in our laboratory as previously published [11]. Primary quantification of positive silver stain (black precipitate) was carried out for the hippocampal and cerebellar regions. Digital photomicrographs were taken at 20× (hippocampus) or 10× (cerebellum) magnification with a Zeiss ImagerA2 microscope and AxioCam mRc5 camera (Zeiss' US subsidiary, Dublin, CA). Photomicrographs were montaged using Neurolucida software (MicroBrightField, Inc, Colchester, VT). Photomicrographs were taken of all brains with fixed exposure settings to ensure consistency. A densitometric quantitative analysis was performed on all silver stain tissue using ImageJ software (1.48v, NIH, Bethesda, MD). Specific regions of interest (dentate gyrus (DG) and the Cornu Ammonis fields 1-3 (CA1-3) in the dorsal hippocampus were traced using strict anatomical borders (Bregma A/P -2.40 mm to -4.68 mm, Fig. 1 [35]) while full coronal cerebellar sections were analyzed (Bregma A/P -12.36 mm to -12.84 mm, Fig. 2 [35]). Digital thresholds of greyscale images separated positive-stained pixels from unstained pixels. Images were segmented into black and white pixels which indicated posi-

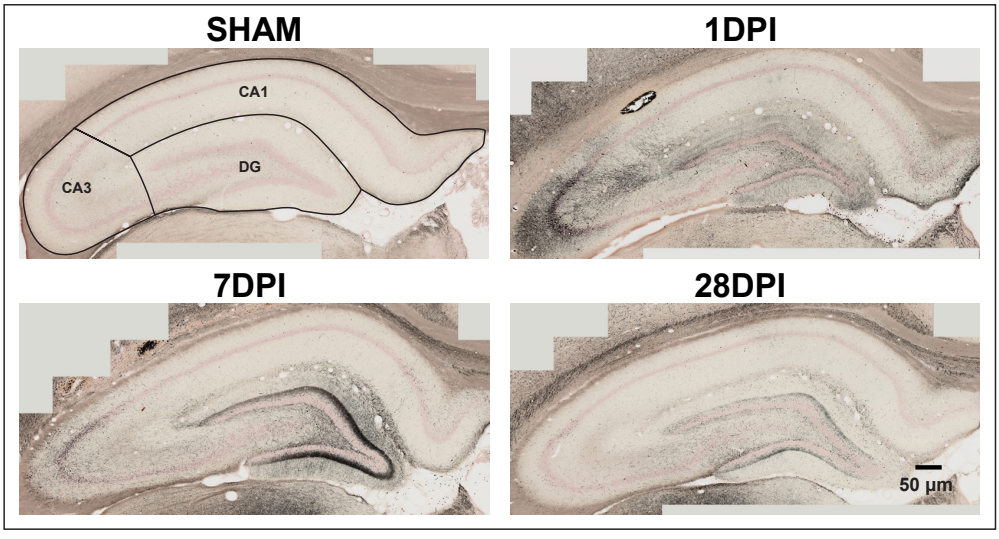

Fig. 1. Representative images show neuropathology in the hippocampus following diffuse TBI that is not present in sham animals. CA1, CA3, and DG were isolated for analyses as overlaid in the sham image. Images from coronal sections were montaged to include the entire hippocampus in the analysis. Scale bar 50 μm for representative images.

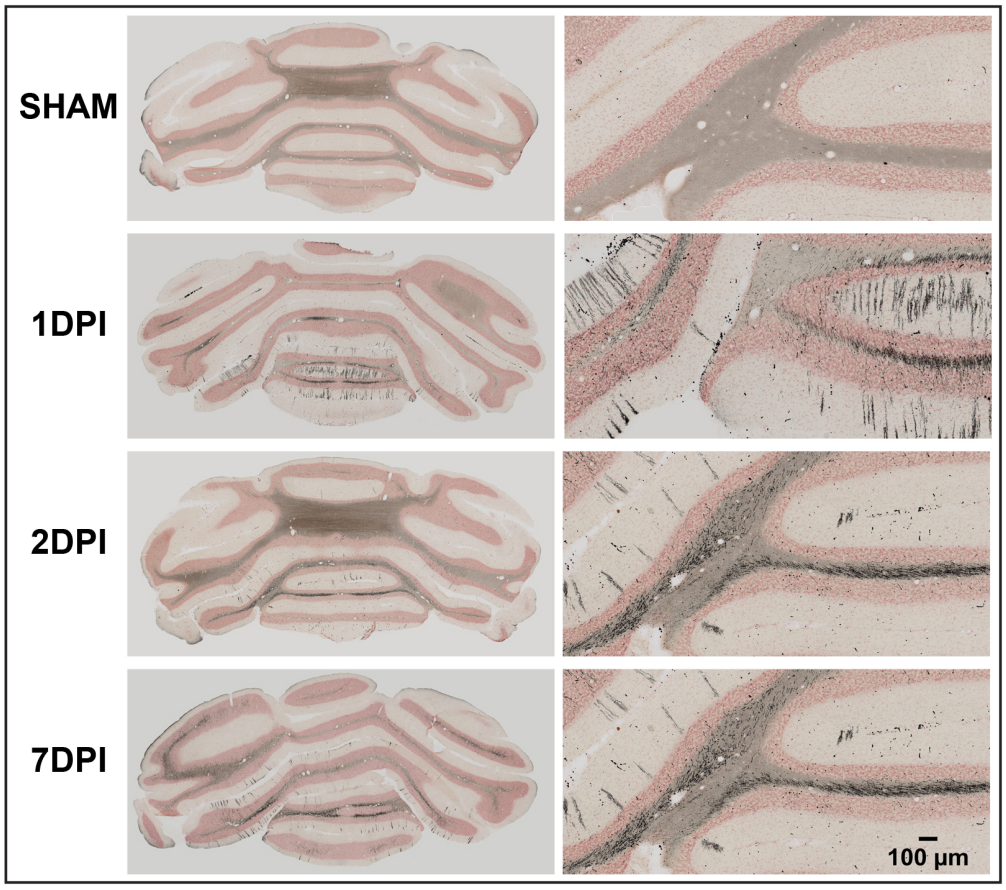

Fig. 2. The cerebellum was montaged for analysis of neuropathology. High magnification representative images show stripes of neuropathology visible in the molecular layer of the cerebellar cortex following diffuse TBI that are not present in sham animals. Additional neuropathology is visible in cerebellar white matter tracts. Images from coronal sections were montaged to include full coronal cerebellar sections in the analysis. Scale bar 100 μm for representative images.

tive and negative staining, and the percentage of positive pixels was calculated within the regions of interest.

Statistical analysis

Previous studies have shown no accumulation of silver stain in sham animals after isoflurane exposure [36-38]. Therefore, in order to reduce the number of animals used in the study, 1 sham animal was collected at each time point while 3 brain-injured animals were collected at each time point. To avoid violating statistical assumptions, one-way analysis of variance (ANOVA) was used to compare neuropathology between all injured rats at the 3 time points post-injury in the hippocampal sub-regions and the cerebellum; sham values were excluded from these analyses. Post hoc comparisons were used and corrected using the Bonferroni method. For comparisons between sham and post-injury time points, independent t-tests were performed for each time point in each region. For the individual t-tests, sphericity was violated for several comparisons. In those cases, a t statistic not assuming homogeneity of variance was computed and reported.

RESULTS

Hippocampal neuropathology microscopy

Several distinct patterns of neuropathology were observed for each hippocampal sub-region over time post-injury (Fig. 1). In the DG, there was observed neuropathology at 1 DPI that increased at 7 DPI. There were several patterns of neuropathology observed in the DG: increased neuropathology in the deep lamina of the granular cell layer, in the ventral and dorsal leaves of the molecular layer, in the polymorphic region, and in the deeper lamina of the granular cell layer at 7 DPI. This pattern of neuropathology is indicative of damage to local and incoming neuronal processes and granular axon terminals. In the CA3 region, neuropathology was observed at all time points and was the only sub-region with neuropathology in the cellular layer. At 1 DPI there was neuropathology in the different strata layers and the pyramidal cellular layer of CA3 that decreased at the subsequent time points. Neuropathology in the CA1 region was observed at the lateral end in the strata and at the transition to the subiculum, most proximal to the impact site.

https://doi.org/10.5607/en21027

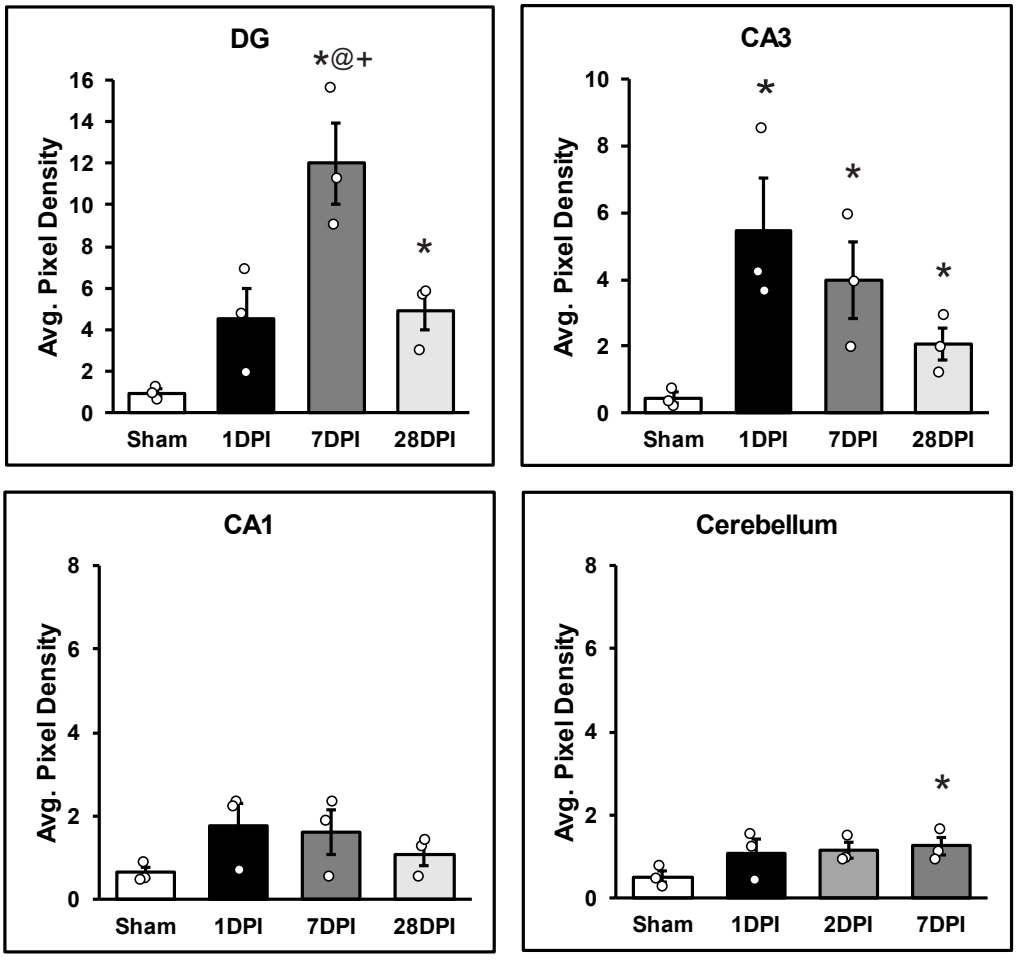

Fig. 3. Quantification of silver accumulation in the DG, CA3 and CA1 hippocampal sub-regions, and the cerebellum. Acute increases in neuropathology were observed at 1 DPI in all sub-regions, and the neuropathology continues to increase in the DG at 7 DPI. By 28 DPI, neuropathology is attenuated and approaches sham levels of silver stained pixels in all hippocampal sub-regions. An increase in neuropathology is observed in cerebellar coronal sections at 7 DPI compared to sham. Note different y-axis for each panel. Data are presented as mean+SEM with statistical significance assigned at $p<0.05$. * indicates significance compared to sham, @ indicates significance compared to 1 DPI, + indicates significance compared to 28 DPI.

Hippocampal neuropathology was increased in a sub-region-specific manner at different time points

A one-way ANOVA was conducted between brain-injured animals for each sub-region. The results revealed a significant effect of time post-injury in the DG ($F(2,8)=8.053$, $p=0.020$; Fig. 3). Post hoc analyses revealed a significant increase in neuropathology at 7 DPI compared to 1 DPI ($p=0.036$) and 28 DPI ($p=0.044$), but no other significant time point comparisons. No main effects were identified for neuropathology in CA3 ($F(2,8)=2.258$, $p=0.186$; Fig. 3) or CA1 ($F(2,8)=0.599$, $p=0.579$; Fig. 3) sub-regions of the dorsal hippocampus.

Independent t-tests for the DG revealed a significant increase in neuropathology in the brain-injured rats compared to sham rats at 7 DPI ($t(4)= 5.689$, $p=0.005$) and 28 DPI ($t(2.144)=4.233$, $p=0.046$), but not at 1 DPI ($t(4)=2.504$, $p=0.066$; Fig. 3). Independent t-tests for the CA3 revealed a significant increase in neuropathology for the brain-injured rats compared to sham rats at all three time points; 1 DPI ($t(4)=3.262$, $p=0.031$), 7 DPI ($t(4)=3.060$, $p=0.038$) and 28 DPI ($t(4)=3.114$, $p=0.036$; Fig. 3). Independent t-tests for the CA1 did not reveal significant increases in neuropathology for the brain-injured rats compared with sham rats at 1 DPI ($t(2.252)=2.083$, $p=0.158$), 7 DPI ($t(4)=1.761$, $p=0.153$) or 28 DPI ($t(4)=1.476$, $p=0.214$; Fig. 3).

Cerebellar neuropathology was increased at 7 days post-injury

Neuropathology was observed almost exclusively in cerebellar white matter tracts and in the molecular layer of the cerebellar cortex in brain-injured rats (Fig. 2). Thin stripes of neuropathology were present throughout the molecular layer of inferior cerebellar lobules (Fig. 2). The superior lobules were generally devoid of neuropathology.

A one-way ANOVA was conducted between the brain-injured animals and revealed no significant effect of time post-injury in the cerebellum ($F(2,8)=0.112$, $p=0.896$; Fig. 3). Independent t-tests were conducted to compare sham to brain-injured neuropathology at each time point. The results revealed no significant differences compared to sham rats at 1 DPI ($t(4)=1.597$, $p=0.185$) or 2 DPI ($t(4)=2.649$, $p=0.057$; Fig. 3). Brain-injured rats had significantly more neuropathology in the cerebellum at 7 DPI compared

to sham rats (t(4)=2.859, p=0.046; Fig. 3).

DISCUSSION

The current study used archived silver stained tissue to extend the quantification of neuropathology following experimental diffuse traumatic brain injury (TBI) into the dorsal hippocampus and cerebellum. Neuropathology in the dorsal hippocampus was sub-region dependent, indicating that the 3 major sub-regions may be exposed to damage and recovery in different ways. Silver staining across the cerebellar cortex and white matter tracts at 7 days post-injury (DPI) confirmed that neuropathology spreads across lobules. Neuropathological findings in this study support the conclusion that all brain regions hold an inherent risk for neuropathology after diffuse TBI. Future studies could include behavioral tasks to associate regional neuropathology and neurological dysfunction after TBI.

The hippocampus is critical for the encoding and retrieval of memories, such that damage to this region may contribute to memory and cognitive deficits [39-46]. Therefore, it is critical to understand the presence and progression of neuropathology in the hippocampus. The hippocampus proper is composed of distinct sub-regions: the dentate gyrus (DG) and the Cornu Ammonis fields 1~3 (CA1~3). These sub-regions form a distinct feed-forward loop that progresses through the DG, CA3, and CA1, sequentially. The current results identify the DG as the most vulnerable to mFPI as evidenced by the largest increase in neuropathology compared to CA1 and CA3. In this study, peak neuropathology occurred between 1 and 7 DPI, with evidence towards resolution by 28 DPI. Substantial cellular turnover occurs in the DG through recruitment of new neurons and elimination of older neurons [47-52], which may be represented among the silver stain observed in this study. The DG is the primary input sub-region for information flowing into the hippocampus from the entorhinal cortex, subiculum and multiple other structures, which may increase DG susceptibility to deafferentation from interconnected regions following a TBI [53-63].

Silver stain techniques detect neuropathology, with limited specificity after TBI. Using alternate markers and techniques, hippocampal sub-regions, specifically the DG, are uniquely vulnerable to neuropathology after TBI. After lateral FPI (mixed focal/diffuse TBI), neuronal cell loss has been reported in sub-regions CA1, CA3, and DG at 7~30 DPI [16, 17, 64, 65] and ipsilateral hippocampal atrophy has been reported out to 12 weeks post-injury [18, 19]. In one study, neuronal cell loss at 7 and 30 DPI was preceded by acute (1 hour to 1 DPI) calcium accumulation and presence of acidophilic neurons in the pyramidal layer of the CA1~3 and the cellular layer of the DG, which indicates specific pathology patterns in sub-regions [64]. Degenerating neurons (Fluoro-Jade positive) in the contralateral DG were observed in higher numbers compared to the contralateral CA1 and CA3; no Fluoro-Jade positive neurons were observed in the hippocampus in either hemisphere at 30 DPI [17], either from recovery or cell loss. An injury severity-dependent decrease in NeuN stained hippocampal neurons has been observed following controlled cortical impact (CCI) [66]. Additionally after CCI, neuropathology (evident by silver stain and Fluoro-Jade) was increased 2 DPI in the contralateral hemisphere with DG neuropathology that resembled the pattern of our results at 7 DPI [36]. Results from these studies, along with our study, showed the primary location of neuropathology in the dorsal hippocampus occurred in the DG. The localization of neuropathology around the cellular layer of the DG indicates that damage may be due to afferent connections from other brain regions that synapse with DG neurons. Future studies are needed to determine the underlying relationship between hippocampal neuropathology and cognitive deficits post-TBI and to investigate neuropathology in sub-regions at more chronic time points.

TBI affects the brain in ways beyond neuropathology. Other pathological processes affect the hippocampus after experimental TBI and extend the sub-region dependent pathology. For example, no changes in the number of astrocytes or oligodendrocytes were reported 14 days after midline or lateral FPI in any hippocampal sub-regions [16]. However, the number of microglia in CA1 was increased after lateral FPI and the number of microglia in CA3 was increased after both lateral and midline FPI which suggests sub-region dependent inflammatory processes at this time point [16]. After mFPI, increased astrocyte reactivity was reported at 30 DPI in the DG and CA1 region compared to sham, but not the CA3 region of the hippocampus [67]. While this same study found no changes in microglia reactivity between sham and mFPI 30 DPI in any hippocampal regions (DG, CA1, CA3), a different study found increased microglia reactivity 30 DPI in DG compared to sham [68]. Inflammation and gliosis may exacerbate neuropathology, or be included within, in hippocampal sub-regions. Pathological processes in the hippocampus can also lead to post-traumatic epilepsy following a TBI [69]. However, epilepsy has been reported after more severe TBI that causes tissue deformation, cell loss, and directly impacts the hippocampus; the prevalence of injury-induced epilepsy after experimental TBI remains low. Overall, diffuse TBI by mFPI results in neuropathology and pathological processes that may disrupt hippocampal function, rather than tissue loss.

The cerebellum is traditionally associated with motor coordination, motor learning, and fine motor control through circuits that include motor cortex and basal ganglia. However, evidence

https://doi.org/10.5607/en21027

suggests additional cerebellar functional roles in the regulation of cognitive and emotional processing [70-72]. The impact of TBI on non-motor cerebellar function has yet to be studied in detail. In a limited number of studies investigating cerebellar pathology after TBI, the molecular layer, containing the Purkinje neuron dendrites, and cerebellar white matter show vulnerability to cerebral cortical TBI, resulting in neuropathology as evidenced with amino cupric silver stain as early as 24 hours and up to 2 weeks post-injury [73]. Neuropathology in the cerebellum has been documented following single and double blast injury and CCI in the rodent where robust silver staining was observed throughout the cerebellar white matter tracts and as distinct thin stripes of silver stain in the molecular layer that line up perpendicular to the dural surface, but no quantitative analyses were reported [73-75]. After mFPI, we quantified similar patterns of silver neuropathology in cerebellar white matter tracts and the molecular layer of the cerebellum and found increased neuropathology at 7 DPI compared to sham. The neuropathology stripes warrant further investigation. While we divided our analyses of the dorsal hippocampus into sub-regions, we analyzed neuropathology in whole coronal sections of the cerebellum. Our cerebellar analyses may have lacked the sensitivity to detect changes in anatomical sub-regions of the cerebellum such as the stripes in the molecular layer or temporal changes in neuropathology in cerebellar white matter tracts. Previous studies from our lab found changes in neuropathology between cerebral cortical layers after mFPI [11]. Future studies should investigate pathological changes in the cerebellum over time by analyzing cerebellar cortical layers independently and should consider quantifying neuropathology beyond 7 DPI.

We quantified silver stained neuropathology to demonstrate cerebellar vulnerability to TBI. Additional studies have observed other pathological markers of post-traumatic injury in the molecular layer of the cerebellar cortex after TBI, which provide further evidence of cerebellar vulnerability. We have previously described the fencing response as a postural reflex after TBI in which the limbs are extended and flexors inhibited upon impact [25]. Axonal pathology and blood brain barrier disruption in the midbrain lateral vestibular nucleus (LVN), adjacent to cerebellar peduncles, suggests that stretching of the cerebellar peduncles upon impact may activate the LVN and result in the observable fencing response [25]. Initial stretching of cerebellar peduncles may cause mechanical damage and changes in neurochemical signaling that explains the delayed (7 DPI) increase of neuropathology that we observed in the cerebellum in this study. Fukuda et al. [76] described stripes of heme oxygenase-1 (HO-1) induction in the vermis of the cerebellum following lateral FPI in rats, suggesting that oxidative stress may play a role in post-traumatic injury of the cerebellum following this injury model [77]. In addition to stripes of silver neuropathology and HO-1 in the cerebellar molecular layer, microglial activation in stripes along the cerebellar cortex has been observed after FPI [78]. Significant Purkinje cell loss occurred following midline FPI at 7 DPI and activated stripes of microglia corresponded to areas of Purkinje cell death in the molecular layer of the cerebellar cortex [78]. The proximity of Purkinje cell death to activated microglial stripes was shown to associate microglia activation prior to the loss of Purkinje cells in the cerebellum following lateral FPI [79]. While the exact function of these activated microglial stripes is still unknown, Igarashi et al. additionally showed activated microglia in stripes along regions of Purkinje cell loss following focal TBI (CCI) [66]. Altogether, these data demonstrate the presence of pathology in the cerebellum after TBI and future studies can extend behavioral analysis of non-motor deficits to cerebellar pathology.

For the present publication, archived tissue was analyzed for post-injury neuropathology in new brain regions, which gives rise to internal study limitations. Only male rats were included when the original tissue was collected [11, 33]. However, the vulnerability of different brain regions and the progression of neuropathology may differ in the male and female brain after diffuse TBI. After a moderate impact-acceleration TBI, male mice had a higher percentage of silver-stained neuropathology throughout the brain compared to female mice [80]. Additionally, neuropathology peaked at 3 DPI in male mice and 14 DPI in female mice, indicating sex-specific neuropathology time courses perhaps dues to endogenous estrogen levels [80]. After CCI, male mice had significantly larger lesions compared to female mice [81], interpreted as the female brain with greater resilience to pathology after TBI. Altogether, including sex as a biological variable in a replication of this study may uncover differential timing and magnitude of neuropathology in the dorsal hippocampus and cerebellum after mFPI. Additionally, archived tissue included different time courses among the brain regions, where the dorsal hippocampus was evaluated out to 28 DPI and the cerebellum was evaluated to 7 DPI. While the time courses do match motor and cognitive deficits observed after mFPI, additional studies are warranted to investigate chronic changes in neuropathology in the cerebellum. Additionally, the role of the cerebellum in cognitive deficits after TBI warrants investigation [7, 82].

Diffuse experimental TBI produces pathology in different brain regions. Our results indicate that different regions are susceptible to different patterns and time courses of neuropathology and may differ within distinct sub-regions of a structure (e.g., dorsal hippocampus, molecular layer of the cerebellum). While the hippocampus is not the only region involved in learning and memory,

a damaged hippocampus can significantly impair memory processes and impede learning while the rest of the brain remains intact [40, 42, 45, 46, 62, 83]. Similarly, the cerebellum is vulnerable to indirect injury processes that could further impair motor, cognitive, or other neurological functions after TBI [84]. These results complement our previous reports of neuropathology after mFPI in the cortex, thalamus, and brain stem which also exhibited a time course for neuropathology that increases over the first 1 to 7 DPI and then starts to normalize at 28 DPI [11, 29, 32-34]. The substantia nigra was the only structure that exhibited sustained neuropathology through 28 DPI after mFPI [33]. Though, this report and our previous reports investigating diffuse neuropathology over time have been primarily conducted in male rats. It is imperative to include female rats in future studies. Understanding the timeline of neuropathology throughout regions of brain following TBI could be critical for therapeutic intervention.

ACKNOWLEDGEMENTS

RKR was an employee at Phoenix Children's Hospital and the University of Arizona College of Medicine – Phoenix at the time the study was conducted.

FUNDING

This work was supported, in part, by Phoenix Children's Hospital Mission Support funds, the Arizona Alzheimer's Consortium, and the Fraternal Order of Eagles. KRG was supported by the National Institute of Neurological Disorders and Stroke of the NIH under award number F31 NS113408.

CONFLICT OF INTEREST

The authors report no conflicts of interest.

DATA AVAILABILITY

Access to data presented in the manuscript is available upon request.

REFERENCES

1. Faul M, Xu L, Wald MM, Coronado VG (2010) Traumatic brain injury in the United States: emergency department visits, hospitalizations and deaths 2002–2006. Centers for Disease Control and Prevention, National Center for Injury Prevention and Control, Atlanta, GA.
2. Blennow K, Brody DL, Kochanek PM, Levin H, McKee A, Ribbers GM, Yaffe K, Zetterberg H (2016) Traumatic brain injuries. Nat Rev Dis Primers 2:16084.
3. Xiong Y, Mahmood A, Chopp M (2013) Animal models of traumatic brain injury. Nat Rev Neurosci 14:128-142.
4. King NS, Crawford S, Wenden FJ, Moss NE, Wade DT (1995) The Rivermead Post Concussion Symptoms Questionnaire: a measure of symptoms commonly experienced after head injury and its reliability. J Neurol 242:587-592.
5. Collins MW, Kontos AP, Reynolds E, Murawski CD, Fu FH (2014) A comprehensive, targeted approach to the clinical care of athletes following sport-related concussion. Knee Surg Sports Traumatol Arthrosc 22:235-246.
6. Brown JA, Dalecki M, Hughes C, Macpherson AK, Sergio LE. Cognitive-motor integration deficits in young adult athletes following concussion. BMC Sports Sci Med Rehabil 2015;7:25.
7. Lifshitz J, Rowe RK, Griffiths DR, Evilsizor MN, Thomas TC, Adelson PD, McIntosh TK (2016) Clinical relevance of midline fluid percussion brain injury: acute deficits, chronic morbidities and the utility of biomarkers. Brain Inj 30:1293-1301.
8. Johnson VE, Stewart W, Smith DH (2013) Axonal pathology in traumatic brain injury. Exp Neurol 246:35-43.
9. Sharp DJ, Scott G, Leech R (2014) Network dysfunction after traumatic brain injury. Nat Rev Neurol 10:156-166.
10. Switzer RC 3rd (2000) Application of silver degeneration stains for neurotoxicity testing. Toxicol Pathol 28:70-83.
11. Lifshitz J, Lisembee AM (2012) Neurodegeneration in the somatosensory cortex after experimental diffuse brain injury. Brain Struct Funct 217:49-61.
12. de Olmos JS (1969) A cupric-silver method for impregnation of terminal axon degeneration and its further use in staining granular argyrophilic neurons. Brain Behav Evol 2:213-237.
13. Ramón y Cajal S (1904) Quelques méthodes de coloration des cylindres, axes, des neurofibrilles et des nids nerveux. Trav Lab Rech Biol 3:1-7.
14. Bielschowsky M (1904) Die silberimpragnation der neurofibrillen. J Psychol Neurol 3:169-189.
15. Glees P (1946) Terminal degeneration within the central nervous system as studied by a new silver method. J Neuropathol Exp Neurol 5:54-59.
16. Grady MS, Charleston JS, Maris D, Witgen BM, Lifshitz J (2003) Neuronal and glial cell number in the hippocampus after experimental traumatic brain injury: analysis by stereological estimation. J Neurotrauma 20:929-941.
17. Tran LD, Lifshitz J, Witgen BM, Schwarzbach E, Cohen AS,

Grady MS (2006) Response of the contralateral hippocampus to lateral fluid percussion brain injury. J Neurotrauma 23:1330-1342.
18. Shultz SR, Wright DK, Zheng P, Stuchbery R, Liu SJ, Sashindranath M, Medcalf RL, Johnston LA, Hovens CM, Jones NC, O'Brien TJ (2015) Sodium selenate reduces hyperphosphorylated tau and improves outcomes after traumatic brain injury. Brain 138(Pt 5):1297-1313.
19. Johnstone VP, Wright DK, Wong K, O'Brien TJ, Rajan R, Shultz SR (2015) Experimental traumatic brain injury results in long-term recovery of functional responsiveness in sensory cortex but persisting structural changes and sensorimotor, cognitive, and emotional deficits. J Neurotrauma 32:1333-1346.
20. Kilkenny C, Browne WJ, Cuthill IC, Emerson M, Altman DG (2010) Improving bioscience research reporting: the ARRIVE guidelines for reporting animal research. PLoS Biol 8:e1000412.
21. Cao T, Thomas TC, Ziebell JM, Pauly JR, Lifshitz J (2012) Morphological and genetic activation of microglia after diffuse traumatic brain injury in the rat. Neuroscience 225:65-75.
22. Lifshitz J, Kelley BJ, Povlishock JT (2007) Perisomatic thalamic axotomy after diffuse traumatic brain injury is associated with atrophy rather than cell death. J Neuropathol Exp Neurol 66:218-229.
23. McNamara KC, Lisembee AM, Lifshitz J (2010) The whisker nuisance task identifies a late-onset, persistent sensory sensitivity in diffuse brain-injured rats. J Neurotrauma 27:695-706.
24. Thomas TC, Hinzman JM, Gerhardt GA, Lifshitz J (2012) Hypersensitive glutamate signaling correlates with the development of late-onset behavioral morbidity in diffuse brain-injured circuitry. J Neurotrauma 29:187-200.
25. Hosseini AH, Lifshitz J (2009) Brain injury forces of moderate magnitude elicit the fencing response. Med Sci Sports Exerc 41:1687-1697.
26. DeOlmos JS, Ingram WR (1971) An improved cupric-silver method for impregnation of axonal and terminal degeneration. Brain Res 33:523-529.
27. de Olmos JS, Beltramino CA, de Olmos de Lorenzo S (1994) Use of an amino-cupric-silver technique for the detection of early and semiacute neuronal degeneration caused by neurotoxicants, hypoxia, and physical trauma. Neurotoxicol Teratol 16:545-561.
28. Mikics E, Baranyi J, Haller J (2008) Rats exposed to traumatic stress bury unfamiliar objects--a novel measure of hypervigilance in PTSD models? Physiol Behav 94:341-348.
29. Miremami JD, Talauliker PM, Harrison JL, Lifshitz J (2014) Neuropathology in sensory, but not motor, brainstem nuclei of the rat whisker circuit after diffuse brain injury. Somatosens Mot Res 31:127-135.
30. Hoffman AN, Paode PR, May HG, Ortiz JB, Kemmou S, Lifshitz J, Conrad CD, Currier Thomas T (2017) Early and persistent dendritic hypertrophy in the basolateral amygdala following experimental diffuse traumatic brain injury. J Neurotrauma 34:213-219.
31. Rowe RK, Rumney BM, May HG, Permana P, Adelson PD, Harman SM, Lifshitz J, Thomas TC (2016) Diffuse traumatic brain injury affects chronic corticosterone function in the rat. Endocr Connect 5:152-166.
32. Thomas TC, Ogle SB, Rumney BM, May HG, Adelson PD, Lifshitz J (2018) Does time heal all wounds? Experimental diffuse traumatic brain injury results in persisting histopathology in the thalamus. Behav Brain Res 340:137-146.
33. van Bregt DR, Thomas TC, Hinzman JM, Cao T, Liu M, Bing G, Gerhardt GA, Pauly JR, Lifshitz J (2012) Substantia nigra vulnerability after a single moderate diffuse brain injury in the rat. Exp Neurol 234:8-19.
34. Ziebell JM, Rowe RK, Harrison JL, Eakin KC, Colburn T, Willyerd FA, Lifshitz J (2016) Experimental diffuse brain injury results in regional alteration of gross vascular morphology independent of neuropathology. Brain Inj 30:217-224.
35. Paxinos G, Watson C (2006) The rat brain in stereotaxic coordinates. 6th ed. Academic Press, Cambridge, MA.
36. Hall ED, Bryant YD, Cho W, Sullivan PG (2008) Evolution of post-traumatic neurodegeneration after controlled cortical impact traumatic brain injury in mice and rats as assessed by the de Olmos silver and fluorojade staining methods. J Neurotrauma 25:235-247.
37. Shitaka Y, Tran HT, Bennett RE, Sanchez L, Levy MA, Dikranian K, Brody DL (2011) Repetitive closed-skull traumatic brain injury in mice causes persistent multifocal axonal injury and microglial reactivity. J Neuropathol Exp Neurol 70:551-567.
38. Rowe RK, Harrison JL, Morrison HW, Subbian V, Murphy SM, Lifshitz J (2019) Acute post-traumatic sleep may define vulnerability to a second traumatic brain injury in mice. J Neurotrauma 36:1318-1334.
39. Albasser MM, Poirier GL, Warburton EC, Aggleton JP (2007) Hippocampal lesions halve immediate-early gene protein counts in retrosplenial cortex: distal dysfunctions in a spatial memory system. Eur J Neurosci 26:1254-1266.
40. Butterly DA, Petroccione MA, Smith DM (2012) Hippocampal context processing is critical for interference free recall of

odor memories in rats. Hippocampus 22:906-913.
41. Eichenbaum H (2004) Hippocampus: cognitive processes and neural representations that underlie declarative memory. Neuron 44:109-120.
42. Scoville WB, Milner B (1957) Loss of recent memory after bilateral hippocampal lesions. J Neurol Neurosurg Psychiatry 20:11-21.
43. Aggleton JP, Brown MW (2005) Contrasting hippocampal and perirhinal cortex function using immediate early gene imaging. Q J Exp Psychol B 58:218-233.
44. Calais JB, Valvassori SS, Resende WR, Feier G, Athié MC, Ribeiro S, Gattaz WF, Quevedo J, Ojopi EB (2013) Long-term decrease in immediate early gene expression after electroconvulsive seizures. J Neural Transm (Vienna) 120:259-266.
45. Bouffard JP, Jarrard LE (1988) Acquisition of a complex place task in rats with selective ibotenate lesions of hippocampal formation: combined lesions of subiculum and entorhinal cortex versus hippocampus. Behav Neurosci 102:828-834.
46. Murray EA, Mishkin M (1998) Object recognition and location memory in monkeys with excitotoxic lesions of the amygdala and hippocampus. J Neurosci 18:6568-6582.
47. Gould E, Beylin A, Tanapat P, Reeves A, Shors TJ (1999) Learning enhances adult neurogenesis in the hippocampal formation. Nat Neurosci 2:260-265.
48. Kempermann G, Kuhn HG, Gage FH (1997) More hippocampal neurons in adult mice living in an enriched environment. Nature 386:493-495.
49. Lim DA, Alvarez-Buylla A (1999) Interaction between astrocytes and adult subventricular zone precursors stimulates neurogenesis. Proc Natl Acad Sci U S A 96:7526-7531.
50. Lois C, Alvarez-Buylla A (1993) Proliferating subventricular zone cells in the adult mammalian forebrain can differentiate into neurons and glia. Proc Natl Acad Sci U S A 90:2074-2077.
51. Gould E, Reeves AJ, Fallah M, Tanapat P, Gross CG, Fuchs E (1999) Hippocampal neurogenesis in adult old world primates. Proc Natl Acad Sci U S A 96:5263-5267.
52. Altman J (1962) Are new neurons formed in the brains of adult mammals? Science 135:1127-1128.
53. Borowsky IW, Collins RC (1989) Histochemical changes in enzymes of energy metabolism in the dentate gyrus accompany deafferentation and synaptic reorganization. Neuroscience 33:253-262.
54. Prins ML, Povlishock JT, Phillips LL (2003) The effects of combined fluid percussion traumatic brain injury and unilateral entorhinal deafferentation on the juvenile rat brain. Brain Res Dev Brain Res 140:93-104.
55. Almaguer-Melian W, Rosillo JC, Frey JU, Bergado JA (2006) Subcortical deafferentation impairs behavioral reinforcement of long-term potentiation in the dentate gyrus of freely moving rats. Neuroscience 138:1083-1088.
56. Janz P, Savanthrapadian S, Häussler U, Kilias A, Nestel S, Kretz O, Kirsch M, Bartos M, Egert U, Haas CA (2017) Synaptic remodeling of entorhinal input contributes to an aberrant hippocampal network in temporal lobe epilepsy. Cereb Cortex 27:2348-2364.
57. Amaral DG, Scharfman HE, Lavenex P (2007) The dentate gyrus: fundamental neuroanatomical organization (dentate gyrus for dummies). Prog Brain Res 163:3-22.
58. Senzai Y (2019) Function of local circuits in the hippocampal dentate gyrus-CA3 system. Neurosci Res 140:43-52.
59. Scharfman HE (2007) The dentate gyrus: a comprehensive guide to structure, function, and clinical implications. Elsevier, Amsterdam.
60. Bayer SA, Altman J (1974) Hippocampal development in the rat: cytogenesis and morphogenesis examined with autoradiography and low-level X-irradiation. J Comp Neurol 158:55-79.
61. Aggleton JP, Vann SD, Saunders RC (2005) Projections from the hippocampal region to the mammillary bodies in macaque monkeys. Eur J Neurosci 22:2519-2530.
62. Jenkins TA, Amin E, Brown MW, Aggleton JP (2006) Changes in immediate early gene expression in the rat brain after unilateral lesions of the hippocampus. Neuroscience 137:747-759.
63. Aggleton JP, O'Mara SM, Vann SD, Wright NF, Tsanov M, Erichsen JT (2010) Hippocampal-anterior thalamic pathways for memory: uncovering a network of direct and indirect actions. Eur J Neurosci 31:2292-2307.
64. Cortez SC, McIntosh TK, Noble LJ (1989) Experimental fluid percussion brain injury: vascular disruption and neuronal and glial alterations. Brain Res 482:271-282.
65. Witgen BM, Lifshitz J, Smith ML, Schwarzbach E, Liang SL, Grady MS, Cohen AS (2005) Regional hippocampal alteration associated with cognitive deficit following experimental brain injury: a systems, network and cellular evaluation. Neuroscience 133:1-15.
66. Igarashi T, Potts MB, Noble-Haeusslein LJ (2007) Injury severity determines Purkinje cell loss and microglial activation in the cerebellum after cortical contusion injury. Exp Neurol 203:258-268.
67. Muccigrosso MM, Ford J, Benner B, Moussa D, Burnsides C, Fenn AM, Popovich PG, Lifshitz J, Walker FR, Eiferman DS, Godbout JP (2016) Cognitive deficits develop 1month

after diffuse brain injury and are exaggerated by microglia-associated reactivity to peripheral immune challenge. Brain Behav Immun 54:95-109.
68. Fenn AM, Gensel JC, Huang Y, Popovich PG, Lifshitz J, Godbout JP (2014) Immune activation promotes depression 1 month after diffuse brain injury: a role for primed microglia. Biol Psychiatry 76:575-584.
69. Shultz SR, Cardamone L, Liu YR, Hogan RE, Maccotta L, Wright DK, Zheng P, Koe A, Gregoire MC, Williams JP, Hicks RJ, Jones NC, Myers DE, O'Brien TJ, Bouilleret V (2013) Can structural or functional changes following traumatic brain injury in the rat predict epileptic outcome? Epilepsia 54:1240-1250.
70. Glickstein M (2007) What does the cerebellum really do? Curr Biol 17:R824-R827.
71. Manto M, Bower JM, Conforto AB, Delgado-García JM, da Guarda SN, Gerwig M, Habas C, Hagura N, Ivry RB, Mariën P, Molinari M, Naito E, Nowak DA, Oulad Ben Taib N, Pelisson D, Tesche CD, Tilikete C, Timmann D (2012) Consensus paper: roles of the cerebellum in motor control--the diversity of ideas on cerebellar involvement in movement. Cerebellum 11:457-487.
72. Schmahmann JD (2019) The cerebellum and cognition. Neurosci Lett 688:62-75.
73. Garman RH, Jenkins LW, Switzer RC 3rd, Bauman RA, Tong LC, Swauger PV, Parks SA, Ritzel DV, Dixon CE, Clark RS, Bayir H, Kagan V, Jackson EK, Kochanek PM (2011) Blast exposure in rats with body shielding is characterized primarily by diffuse axonal injury. J Neurotrauma 28:947-959.
74. Calabrese E, Du F, Garman RH, Johnson GA, Riccio C, Tong LC, Long JB (2014) Diffusion tensor imaging reveals white matter injury in a rat model of repetitive blast-induced traumatic brain injury. J Neurotrauma 31:938-950.
75. Wiley CA, Bissel SJ, Lesniak A, Dixon CE, Franks J, Beer Stolz D, Sun M, Wang G, Switzer R, Kochanek PM, Murdoch G (2016) Ultrastructure of diaschisis lesions after traumatic brain injury. J Neurotrauma 33:1866-1882.
76. Fukuda K, Richmon JD, Sato M, Sharp FR, Panter SS, Noble LJ (1996) Induction of heme oxygenase-1 (HO-1) in glia after traumatic brain injury. Brain Res 736:68-75.
77. Sato M, Noble LJ (1998) Involvement of the endothelin receptor subtype A in neuronal pathogenesis after traumatic brain injury. Brain Res 809:39-49.
78. Mautes AE, Fukuda K, Noble LJ (1996) Cellular response in the cerebellum after midline traumatic brain injury in the rat. Neurosci Lett 214:95-98.
79. Fukuda K, Aihara N, Sagar SM, Sharp FR, Pitts LH, Honkaniemi J, Noble LJ (1996) Purkinje cell vulnerability to mild traumatic brain injury. J Neurotrauma 13:255-266.
80. Kupina NC, Detloff MR, Bobrowski WF, Snyder BJ, Hall ED (2003) Cytoskeletal protein degradation and neurodegeneration evolves differently in males and females following experimental head injury. Exp Neurol 180:55-73.
81. Gölz C, Kirchhoff FP, Westerhorstmann J, Schmidt M, Hirnet T, Rune GM, Bender RA, Schäfer MKE (2019) Sex hormones modulate pathogenic processes in experimental traumatic brain injury. J Neurochem 150:173-187.
82. Liang KJ, Carlson ES (2020) Resistance, vulnerability and resilience: a review of the cognitive cerebellum in aging and neurodegenerative diseases. Neurobiol Learn Mem 170:106981.
83. Milner B, Klein D (2016) Loss of recent memory after bilateral hippocampal lesions: memory and memories-looking back and looking forward. J Neurol Neurosurg Psychiatry 87:230.
84. Park E, Ai J, Baker AJ (2007) Cerebellar injury: clinical relevance and potential in traumatic brain injury research. Prog Brain Res 161:327-338.